

# THE INFLUENCE OF GEOMETRY ON THE ENERGY ABSORPTION CAPABILITY OF COMPOSITE STRUCTURES MADE OF WOVEN FABRIC PREPREGS

Mehmet C. Engül<sup>1</sup>, Serdar Demir<sup>1</sup> and Nuri Ersoy<sup>1</sup>

<sup>1</sup>Boğaziçi University, Department of Mechanical Engineering 34342 Bebek/Istanbul TURKEY, mehmet.engul@boun.edu.tr, <http://www.composites.boun.edu.tr>

**Keywords:** Composites, Woven prepregs, Specific Energy Absorption, Sinusoidal Geometry, FEA

## ABSTRACT

While composite structures have superior performance related to energy absorption, failure mechanisms for various geometries occurring during the crushing process and their influence on Specific Energy Absorption (SEA) are still unclear. Therefore, there is a requirement for a systematic study to investigate the influence of geometry on SEA, starting from simple geometries to more complex structures. This paper presents both experimental and numerical investigations of the crushing process for structures made of woven fabric prepregs including flat coupons and sinusoidal geometries with different diameters and number of curvatures. In numerical analysis, a Finite Element (FE) modelling approach is developed in order to predict crushing behaviour of tested composite structures. Results are discussed and compared in terms of the observed failure mechanisms.

## 1 INTRODUCTION

CFRP composites are being increasingly used in the industry because of their benefits over metallic materials including superior performance related to energy absorption during crash events. However, the amount of energy absorbed by a composite structure is not easily predicted due to the complexity of the crush induced failure mechanisms that involve not only in-plane, but also the interlaminar damage. Especially, the integrated structure of woven composites with interlocking tow architectures makes this estimation more difficult. From 1980s to present, there is a comprehensive literature about the energy absorption capability of composite materials.

The view commonly shared by the researchers is that there are several different failure modes occurring simultaneously during the crush event (splaying, fragmentation, and delamination, etc.), each of which contributes to the energy absorption capability [1-4]. It is also known that there are several factors such as material system, fibre orientation, trigger mechanisms, etc. which are affecting the order and the intensity of these failure modes; however, there is no clear consensus on exactly how this influence is exerted.

Recently, the interest in composite coupon level tests is increasing since flat plates are easy to manufacture while providing a standardization so that the influence of parameters on energy absorption capability can be systematically compared [5-9]. Besides flat plates, it is still important to study the energy absorption of complex structures since geometry has also a major influence on SEA. Although most of the previous studies have focused on tubular specimens [10-12], it is known that corrugated designs such as sinusoidal geometries improve the energy absorption capability to a considerable extent [13-15]. However, among the numerous studies focusing on the crashworthiness of complex composite geometries, there is a limited number of works conducting a systematic study to understand the influence of geometry on energy absorption capability, starting from flat plates to complex structures. Engül et al. [16] recently conducted a holistic study investigating the influence of geometry on the SEA of composite structures made of carbon fibre/epoxy unidirectional (UD) prepregs through various geometries such as flat plate, semi-circle, and sinusoidal specimens. Moreover, the variation of failure modes for different geometries and their contribution to the SEA values were discussed in detail.

When it comes to composite structures made of woven prepregs, a further investigation is still required to understand the change of failure modes with different geometries and the relationship between these modes and the amount of absorbed energy. In this paper, the influence of geometry on the SEA of composite structures manufactured from a carbon fibre/epoxy woven fabric prepregs are investigated through flat plate and sinusoidal geometries. By keeping the cross-sectional area (thus weight) constant, sinusoidal structures with different number of curvatures and diameter sizes are tested. In addition to experimental tests, FE models are developed in Abaqus/Explicit for sinusoidal structures to estimate SEA numerically. The results are compared and discussed in terms of failure mechanisms occurring during the process and their contribution to the SEA.

## 2 EXPERIMENTAL

The flat coupon plates are manufactured from prepregs supplied by KORDSA with product code KOM10T/PL200, which is a carbon-epoxy plain weave fabric (WF) preprep composed of Toray T300 (3K) yarns impregnated with OM10 resin. 8 plies of WF prepregs are stacked on the flat steel mold and vacuum bagged. The manufacturing process is carried out in the autoclave according to the Manufacturer’s Recommended Cure Cycle [17]. 300 mm x 300 mm plates thus manufactured are then cut by a diamond disk cutter into final test coupons. The upper edge of the coupon is chamfered to ensure progressive failure by delamination initiation and prevent catastrophic damage. A simple fixture with 50 mm support length is designed to avoid buckling. The illustration of the fixture and the specimen with chamfered edge are presented in Fig. 1.

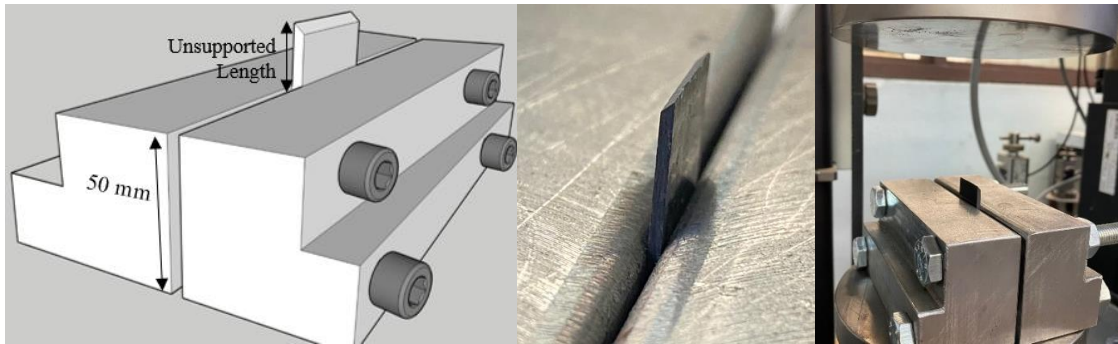


Figure 1: The illustration of the supporting fixture (left), the specimen (middle), and test setup (right).

The determination of the unsupported length is significant as it may cause buckling if the dimension is higher than a certain critical value. According to some researchers [8,18], the unsupported length to thickness ratio should vary between 2 and 4. To ensure the stabilization around a mean value in load-displacement curve after peak load, the ratio is specified to be approximately 4. Three specimens are tested in the Zwick Z100 testing machine with quasi-static speed of 0.5 mm/min. The dimensions for the flat coupons including the unsupported length are given in Table 1.

Table 1: Dimensions of the flat coupon test samples.

# of plies	Thickness [mm]	Width [mm]	Length [mm]	Unsupported Length [mm]
8	1,6	20	56	6

The design of the sinusoidal structures consists of different number of repeating semi-circle curvatures. The idea is to keep the weight of material used constant while adding more semi-circle curvatures which leads the decrease in radii. So, sinusoidal structure with 3 curvatures (having 15 mm radii) and with 5 curvatures (having 9 mm radii) are manufactured. Both structures have 8 mm straight lips positioned at each end. The schematic of cross sections of the sinusoidal structures with 3 and 5 curvatures can be seen in Fig. 2.

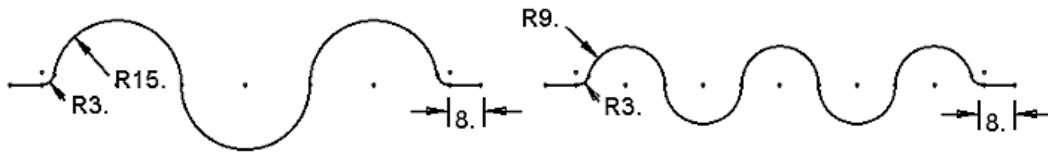


Figure 2: The schematic of the cross sections of sinusoidal structures with 3 curvatures (left), and 5 curvatures (right) (all dimensions are in millimeters.)

The manufacturing process is again carried out in autoclave by stacking 8 plies of WF prepreps on steel molds. Fig. 3 demonstrates the manufactured woven fabric sinusoidal structures. Before proceeding to the testing phase, the specimens were cut to 56 mm in length and the top edges were chamfered at 45° as applied to unidirectional specimens. Weight of the specimens has an average value of 22,26 grams for 56 mm length. Then, three specimens of each geometry are tested in the Zwick Z100 testing machine with quasi-static speed of 0.5 mm/min.

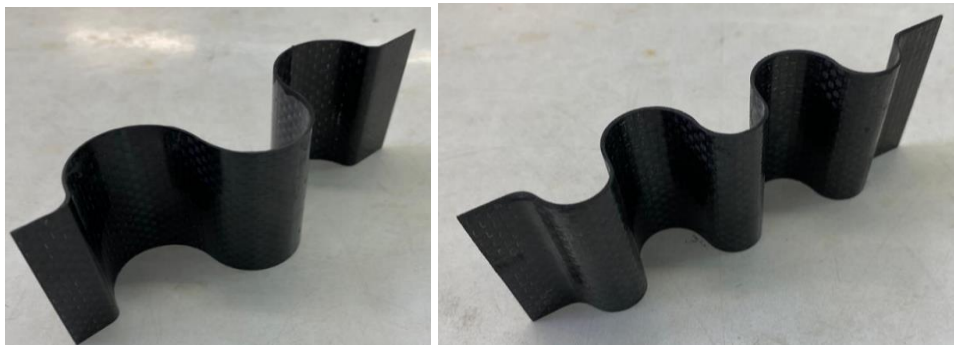


Figure 3: Manufactured sinusoidal specimens with 3 curvatures (left) and 5 curvatures (right).

### 3 NUMERICAL

Axial crushing behavior of the composite specimens are investigated numerically by developing Finite Element (FE) models. Proposed modelling approach is validated first by simulating the sinusoidal structures having 3 and 5 curvatures and comparing the experimental results with numerical results. After validation, sinusoidal structure with 7 curvatures is also modelled to understand how SEA is evolving with increasing number of curvatures while keeping the amount of material constant.

FE models are generated on Abaqus/Explicit commercial FEA software and incorporates both intralaminar and interlaminar damage mechanisms. Eight plies of the woven CFRP structures are generated and meshed individually with continuum shell elements (SC8R). The intralaminar damage is defined by built-in ABQ\_PLY\_FABRIC subroutine material model. The interlaminar damage is modelled with Cohesive Zone Method (CZM).

ABQ\_PLY\_FABRIC subroutine is a material model used to define the intralaminar damage response of fabric reinforced composites. It models each ply as homogeneous orthotropic material which shows progressive stiffness degradation due to fiber/matrix damage [19]. ABQ\_PLY\_FABRIC subroutine contains the constitutive equations that defines orthotropic damaged elasticity, damage initiation and damage evolution. VUMAT for Fabric Reinforced Composites document [19] provides the detailed information of the subroutine. Same material model is also used in various studies in the literature [12, 15].

CFRP woven prepreg used to produce crash structures investigated in this study consists of plain weave 3K T300 carbon fibers manufactured by Toray and the resin system is epoxy resin. Epoxy resin content of the prepregs is 42% by weight. The plain weave composite prepregs have very similar characteristics with the CFRP woven prepregs used by Zhou et al. [12]. Therefore, the material properties provided by Zhou et al. are used in this study. Intralaminar properties of the prepreg are listed in Table 2.

Table 2: Intralaminar damage properties [12].

Property	Symbol	Value	Unit
Density	$\rho$	1.56	g/cm <sup>3</sup>
Young Modulus along fiber direction 1	$E_1$	65.1	GPa
Young Modulus along fiber direction 2	$E_2$	64.4	GPa
Shear Modulus	$G_{12}$	4.5	GPa
Principal Poisson Ratio	$\nu_{12}$	0.037	-
Tensile Strength along fiber direction 1	$X_{1+}$	776	MPa
Compressive Strength along fiber direction 1	$X_{1-}$	704	MPa
Tensile Strength along fiber direction 2	$X_{2+}$	760	MPa
Compressive Strength along fiber direction 2	$X_{2-}$	698	MPa
Shear Stress at the initiation of shear damage	$S$	95	MPa
Tensile fracture energy per unit area along fiber direction 1	$G_f^{1+}$	125	kJ/m <sup>2</sup>
Compressive fracture energy per unit area along fiber direction 1	$G_f^{1-}$	250	kJ/m <sup>2</sup>
Tensile fracture energy per unit area along fiber direction 2	$G_f^{2+}$	95	kJ/m <sup>2</sup>
Compressive fracture energy per unit area along fiber direction 1	$G_f^{2-}$	245	kJ/m <sup>2</sup>
Shear damage equation parameter	$\alpha_{12}$	0.18	-
Max shear damage	$d_{12}^{max}$	0.99	-
Initial effective shear yield stress	$\tilde{\sigma}_{y0}$	185	MPa
Hardening equation coefficient	$C$	1053	-
Hardening equation power term	$p$	0.41	-
Element deletion flag	1DelFlag	1	-
Maximum value of damage variables	$d_{max}$	0.99	-

The interlaminar damage response of the composite structures refers to the delamination of the plies. In axial crushing behavior of composite structures, delamination occurs through a mixed-mode of opening and two shearing modes. CZM is a very convenient method to model the mixed-mode delamination of composite structures. In this study, CZM is applied by defining cohesive interactions between surfaces of the generated plies. These cohesive contact behavior is defined by traction-separation law. The interlaminar response before the damage initiation is considered as linear elastic. Quadratic stress damage initiation criterion is applied to model damage initiation. Damage evolution is modelled with Benzeggagh-Kenane damage evolution law. Interlaminar damage properties used in this study are listed in Table 3. Penalty stiffness values used in the study are selected according to the studies of Turon et al. and Camanho et al. [20, 21]. The detailed information about the damage initiation and evolution values can be obtained from Sokolinsky et al.'s study [15].

Table 3: Interlaminar damage properties [15].

Description	Mode I	Mode II	Mode III	Unit
Penalty Stiffness	$2 \times 10^6$	$1 \times 10^6$	$1 \times 10^6$	N/mm <sup>3</sup>
Damage Initiation	54	70	70	MPa
Fracture Energy	0.504	1.566	1.566	kJ/mm <sup>2</sup>

### 3.1 FE Model of Sinusoidal Structures

The sinusoidal specimens with 3 and 5 curvatures are modeled to compare the simulation results with the experimental results, thus validating the FE modelling approach. The plies of the sinusoidal structures are generated by sweeping the structure layers along the cross-sections shown in Fig. 2. The composite structure models are made of eight plies with a thickness of 0.2 mm each, meshed with approximately  $1.0 \times 1.0$  mm planar continuum shell elements. Sinusoidal structures are connected to a rigid plate at the bottom with tie contacts. Needle type trigger is generated on the top of the structures. Intralaminar properties are defined to the plies by assigning homogeneous continuum shell sections. Sinusoidal structures are modeled as full-scale models with a height of 25 mm. The generated models for 3 and 5 curvature structures are illustrated in Fig. 4. Boundary conditions of the models are shown on the side view of 5 curvature sinusoidal structure in Fig. 5.

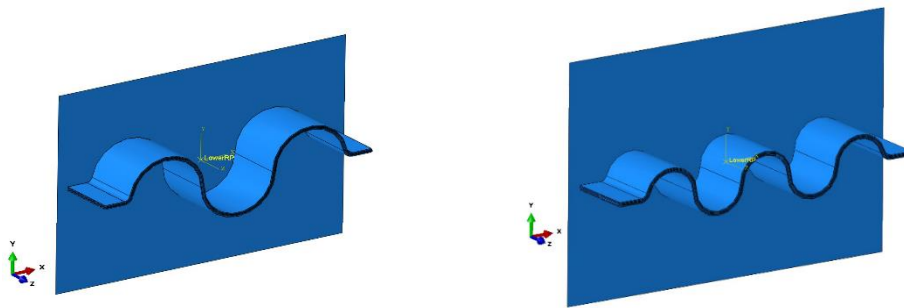


Figure 4: Abaqus/CAE model of the 5 curvature sinusoidal structure; isometric view (left), side view (right).

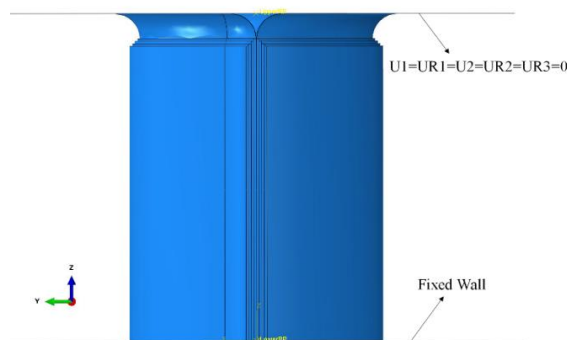


Figure 5: Boundary conditions of the FE models (side-view of the 5 curvature structure).

As can be seen in the side view given in Fig. 5; the upper rigid plate has a V-shape section which represents the artificial-plug initiator, which is used to simulate the debris wedge accumulation that occurs during axial crush. Using a wedge-like plug initiator helps to initiate delamination properly and provides a more stable crushing behavior. It is a convenient method to model the axial crushing behavior of composite structures [22, 23]. The artificial plug-initiator is swept along the cross-sections of the structures given in Fig. 2. The side view schematic of the applied plug-initiator is illustrated in Fig. 6.

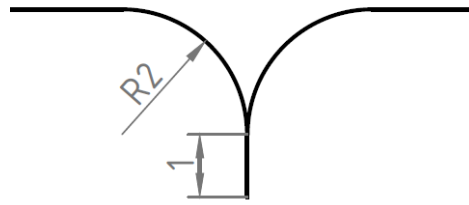


Figure 6: Cross-section of the applied artificial-plug initiator section. (Dimensions are in mm.)

The artificial-plug initiator has a needle-like section which helps to prevent global-buckling and provides more stability in the simulation. Since continuum shell elements are deleted as they reach to the damage criterion, the debris accumulation behavior cannot be simulated correctly [22]. The artificial-plug initiator acts as the debris wedge and provides the simulation to reach a stable progressive crushing behavior.

Rigid parts used in the simulation are meshed with rigid elements (R3D4). Artificial plug initiator section of the upper rigid plate is meshed with approximately  $0.5 \times 0.5$  mm elements. The velocity of the upper rigid part is defined as 1000 mm/s as it is suggested in Zhou et al.'s study [12] to reduce the computational time. It is stated that dynamic effects become significant beyond 500-1000 mm/s crushing velocities [15]. The friction coefficient between composite and rigid parts are defined as 0.2 and the friction coefficient between plies after delamination is defined as 0.3. Friction coefficients are defined with tangential behavior between parts by assigning penalty friction formulation. Also normal behavior defined between parts with hard contact.

### 3.2 FE Model of Sinusoidal Structure with 7 Curvatures

By validating the FE modelling approach with the results of 3- and 5 curvature sinusoidal structures, axial crushing of further complex geometries can be simulated using the same modeling method. In this respect, a sinusoidal structure with 7 curvatures is simulated to investigate the crushing characteristics. Since the amount of the material and its weight are desired to be same with the previously investigated geometries, the radius of the semi-circles are estimated as 6.43 mm. The isometric view of full model and the schematic of the cross-section of the structure is shown in Fig. 7.

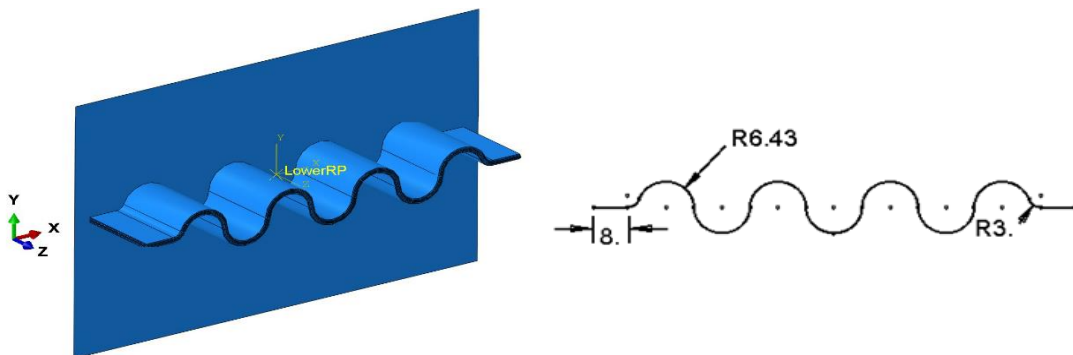


Figure 7: Sinusoidal structure with 7 curvatures; Abaqus/CAE model (left), schematic of the cross-section of the structure (right) (all dimensions given in millimeters).

## 4 RESULTS AND DISCUSSION

### 4.1 Experimental Results of Flat Plate Coupons

Flat test coupon specimens are tested experimentally as described before to observe the failure mechanisms and crushing morphology and to examine the load-displacement curve trends. Fig. 8 demonstrates the load-displacement curves of 8 ply flat plate structures and the crushed morphology of the specimens. SEA results of the flat plate specimen tests are given in Table 4.

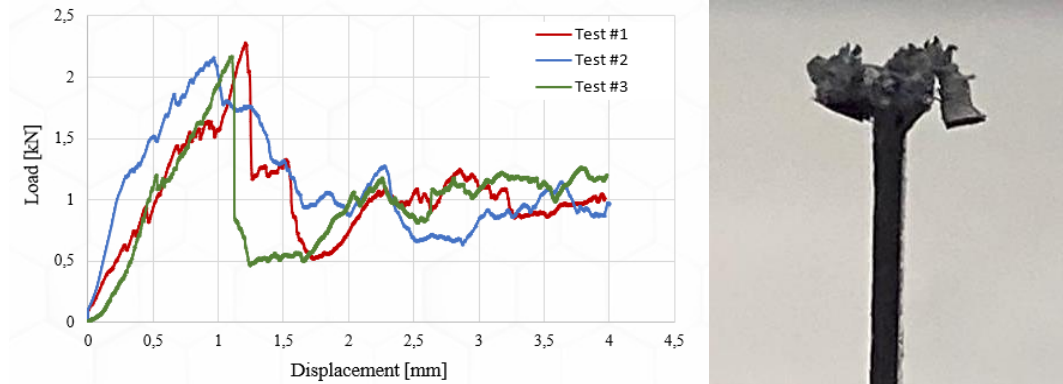


Figure 8: Experimental quasi-static crushing test results of flat plate specimens; load-displacement curves (left), crushed morphology (right).

Table 4: SEA values of the flat plate specimens.

Specimen No	SEA [J/g]	Average
#1	51.75	50.42
#2	51.05	
#3	48.46	

Investigating the crushed morphology of the flat plate specimens, it is observed that after the first delamination occurring at the interface between first and second plies, both matrix cracks and fiber fractures begin to occur directly in the first ply, after a small amount of bending. The fragmentation mode characterized by matrix cracks and fiber failure continue to be seen in the rest of the plies and the debris is formed by these accumulated fragments. The textile nature of woven fabric prepregs obtained by interlocking yarns is the reason why fragmentation mode becomes dominant throughout the process rather than splaying mode.

### 4.2 Experimental Results of Sinusoidal Structures with 3 and 5 Curvatures

Following the investigation axial quasi-static crushing characteristics of flat plate specimens, sinusoidal structures manufactured are tested experimentally. Experimental load-displacement curves of the sinusoidal structures tested are given in Fig. 9 and the crushed morphology of the sinusoidal structures are shown in Fig. 10.

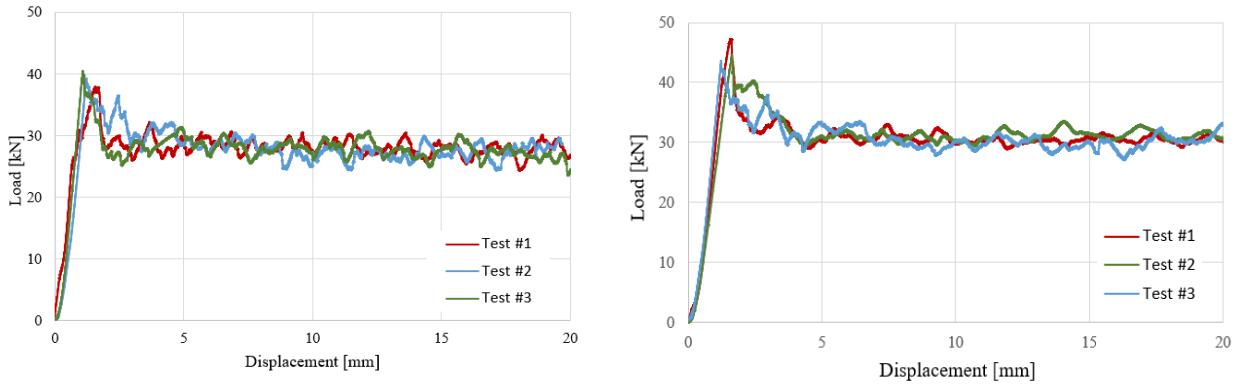


Figure 9: Experimental load-displacement curves of the sinusoidal structures; 3 curvatures (left), 5 curvatures (right).



Figure 10: Crushed morphologies of the sinusoidal structures; 3 curvatures (left), 5 curvatures (right).

According to the observations made during the tests, it can be said that the inflection points between the repeating semi-circle segments create obstacles and prevent plies from splaying and promote vertical fiber ruptures and fragmentation. Moreover, due to having more inflection points, the mean load and the resultant energy absorption performance of sinusoidal structure having 5 curvatures is higher than the sinusoidal structure with 3 curvatures and flat specimens. From the load-displacement results of the experimental tests, the mean load is evaluated as 28,5 kN for sinusoidal structure with 3 curvatures, this value increases to 31,2 kN for sinusoidal structure with 5 curvatures. SEA values obtained from the experimental tests are given in Table 5.

Table 5: SEA values of the sinusoidal structures experimental test results.

Geometry	Specimen No	SEA [J/g]	Average
Sinusoidal (3 Curvatures)	#1	69.84	69.33
	#2	68.94	
	#3	69.20	
Sinusoidal (5 Curvatures)	#1	76.01	76.37
	#2	77.40	
	#3	75.72	

### 4.3 Numerical Results of Sinusoidal Structures

In this section, in order to validate the FE modelling approach, results obtained from the FE models of 3 and 5 curvature sinusoidal structures are evaluated and compared to the experimental results in terms of load-displacement curves, crushing modes and SEA values. Comparison of experimental and numerical load-displacement curves are shown in Fig. 11, which shows that the numerical and experimental curves are very close to each other beyond 4 mm crush displacement. In experimental load-displacement curves, there is a peak load followed by a gradual decrease in load until a stable damage progression zone is reached. The discrepancy before 4 mm displacement is probably due to the action of artificial plug initiator used in the model, which helps delamination initiation resulting underestimation of the peak load before damage starts. Therefore, it can be asserted that the model can predict the crushing characteristics and energy absorption values quite close to the experimental data in the stable damage zone.

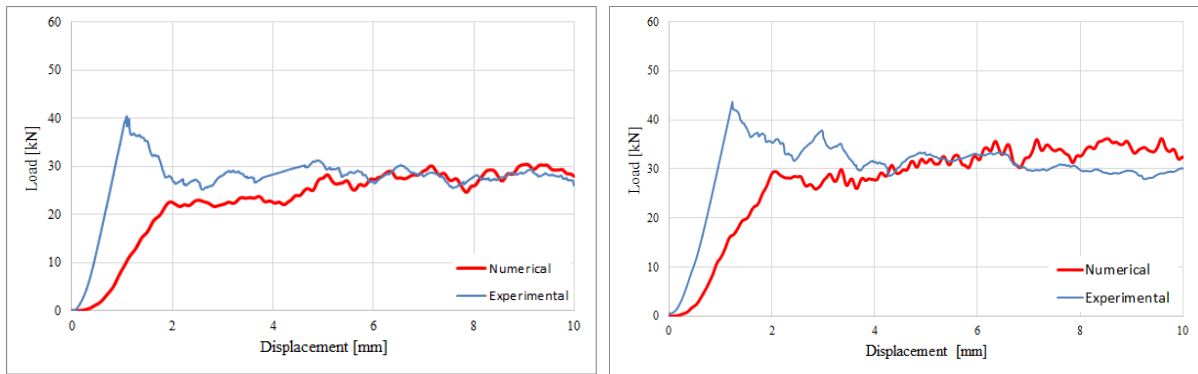


Figure 11: Experimental and numerical load-displacement curves of the sinusoidal structures; 3 curvatures (left) 5 curvatures (right).

Crushed morphologies obtained from FE models and the experiments for sinusoidal structures with 3 and 5 curvatures are given and compared in Fig. 12 and Fig. 13 respectively. It can be stated that, crushed morphologies obtained from FE simulations shown good correlation with the experimental tests results. Vertical tears can be observed on the structure wall and no global buckling occurred on FE model results. For 10 mm crush displacement, SEA values obtained from the simulations are 70.22 J/g for 3 curvature structure and 74.02 J/g for 5 curvature structure. The SEA values obtained through simulation are very close to the experimental values thus it can be stated that the FE modelling approach is quite capable of estimating energy absorption capability of sinusoidal structures.



Figure 12: Crushed morphology of sinusoidal structure with 3 curvature; FE model (left) (red elements are damaged), experimental (right).

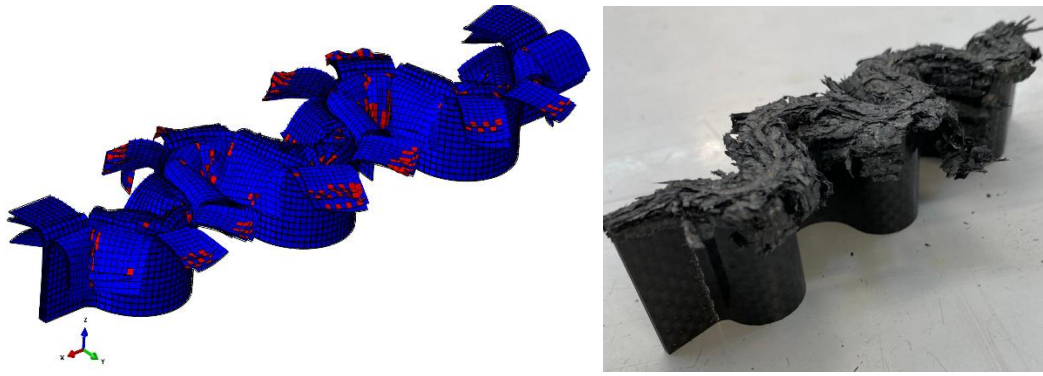


Figure 13: Crushed morphology of sinusoidal structure with 5 curvature; FE model (left) (red elements are damaged), experimental (right).

#### 4.4 Numerical Results of Sinusoidal Structures with 7 Curvatures

Sinusoidal structure with 7 curvatures is modelled with the same approach and the simulated load-displacement curve is given in Figure 14. Apparently, mean crush force in the stable zone is around 37.5 kN.

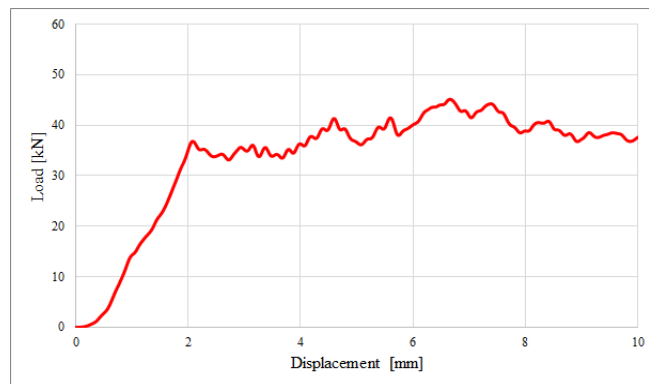


Figure 14: Numerical load-displacement curve of the sinusoidal structure with 7 curvatures.

Crushed morphology obtained from the numerical simulation is given in Figure 15. Again the crushed morphology showed vertical tears and no global-buckling due to the artificial-plug initiator used in modelling. For 10 mm crush displacement, estimated SEA value from the numerical study of 7 structure is 89.47 J/g and this is quite higher than other structures. A summary of all experimentally measured and numerically predicted SEA values for structures examined are given in Figure 16.

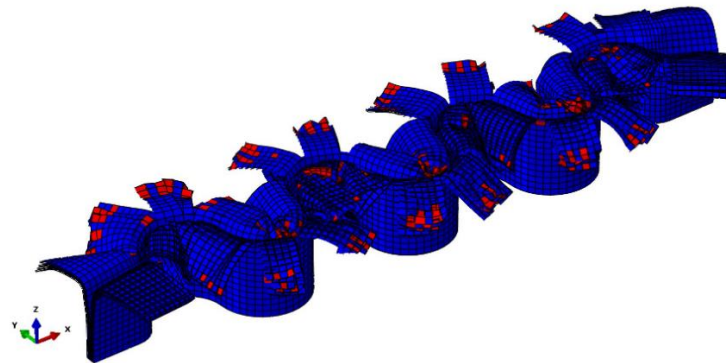


Figure 15: Crushed morphology of the FE model of sinusoidal structure with 7 curvatures.

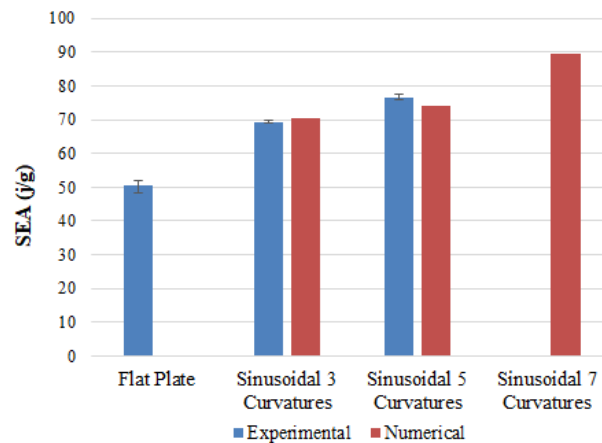


Figure 16. Comparison of the SEA values of the investigated structures.

## 5 CONCLUSIONS

This paper presented both experimental and numerical investigations for the crushing process of flat plates and sinusoidal structures made of a plain weave fabric prepregs of carbon fibre/epoxy resin. The main goal of this study was to understand the influence of geometry on the specific energy absorption, the variation of the crush induced failure mechanisms through various geometries and their contributions to the energy absorption capability. The overall conclusion derived from the experimental results is that the level of fragmentation mode increases as the number of curvatures increase, because as the number of curvatures increase, so as the number of inflection points connecting semicircles, and these serve as obstacles for splaying and increases fragmentation. Therefore, sinusoidal structures have greater potential in terms of energy absorption compared to flat coupon plates. Results show that as the number of semi-circle curvatures increases and the radius of each segment becomes smaller, the SEA increases even though the amount of material remains same.

Another goal of the study was to develop an accurate FE modelling approach for crushing of sinusoidal structures. This goal is achieved by validating the simulation results of 3 and 5 curvature sinusoidal structures with experimental results. Then, 7 curvature sinusoidal structure were modelled with the same approach. The numerical results show that of the 7 curvature structure gives higher energy absorption values than 5 curvature structure. The possible difficulties in the manufacturing process of the sinusoidal structure with 7 curvatures, on the other hand, should also be considered. As a result of the numerical study, even if it gives the highest value, it may not be possible to manufacture a reliable structure since the curvature radius is too small. For this reason, in real-life applications, the structure with 5 curvatures is preferable.

**Funding:** This work was supported by the Boğaziçi University Research Fund with Grant Number 17621D.

## REFERENCES

- [1] G. L. Farley, Energy-absorption capability of composite tubes and beams. PhD Thesis, NASA, Virginia; 1989.
- [2] D. Hull, A unified approach to progressive crushing of fibre-reinforced composite tubes, *Composites Science and Technology*, **40**, 1991, pp. 377-421.

- [3] C. Bisagni, Experimental investigation of the collapse modes and energy absorption characteristics of composite tubes, *International Journal of Crashworthiness*, **4**, 2009, pp. 365-378.
- [4] D. Chen, X. Sun, B. Li, Y. Liu, T. Zhu and S. Xiao, On Crashworthiness and Energy Absorbing Mechanisms of Thick CFRP Structures for Railway Vehicles, *Polymers*, **14**, 2022, p. 4795.
- [5] H. Liu, B. G. Falzon and J. P. Dear, An experimental and numerical study on the crush behaviour of hybrid unidirectional/woven carbon-fibre reinforced composite laminates, *International Journal of Mechanical Sciences*, **164**, 2019, p. 105160.
- [6] H. Israr, S. Rivallant, C. Bouvet and J. Barrau, Finite element simulation of 0°/90° CFRP laminated plates subjected to crushing using a free-face-crushing concept, *Composites Part A: Applied Science and Manufacturing*, **62**, 2014, pp. 16-25.
- [7] P. Feraboli, Development of a Modified Flat-plate Test Specimen and Fixture for Composite Materials Crush Energy Absorption, *Journal of Composite Materials*, **19**, 2009, pp. 1967-1989.
- [8] T. Bru, P. Walderström, R. Gutkin and G. M. Vyas, Development of a Test Method for Evaluating the Crushing Behaviour of Unidirectional Laminates. *Journal of Composite Materials*, **51**, 2017, pp. 1-11.
- [9] M. C. Engül and N. Ersoy, Energy absorption capability of carbon/epoxy composite laminates: A novel numerical approach, *Journal of Reinforced Plastics and Composites*, 2023.
- [10] P. Thornton, Energy absorption in composite structures. *Journal of Composite Materials*, **13**, 1979, 248-262.
- [11] O. Alhyari and G. Newaz, Energy Absorption in Carbon Fiber Composites with Holes, *Journal of Carbon Research*, **7**, 2021, pp. 1-13.
- [12] G. Zhou, G. Sun, G. Li, A. Cheng and Q. Li, Modelling for CFRP structures subjected to quasi-static crushing. *Composite Structures*, **184**, 2018, pp. 41-55.
- [13] S. Hanagud, I. Craig, P. Sriram and W. Zhou, Energy absorption behavior of graphite epoxy composite sine webs. *Journal of Composite Materials*, **23**, 1989, pp. 448-459.
- [14] J. F. M. Wiggensraad, D. Santoro, F. Lepage, C. Kindervater and H. C. Mañez, Development of a crashworthy composite fuselage concept for a commuter aircraft. *NLR-TP*, 2001, p. 108.
- [15] V. Sokolinsky, K. Indermuehle and J. Hurtado, Numerical simulation of the crushing process of a corrugated composite plate. *Composites Part A: Applied Science and Manufacturing*, **42**, 2013, pp. 1119-1126.
- [16] M. Engül and N. Ersoy, From Flat Plates to Sinusoidal Structures: Influence of Geometry on the Energy Absorption Capability of Carbon/Epoxy Composites, *Journal of Composites Science*, **7**, 2023.
- [17] OM10 Resin System Prepregs Technical Data Sheet, KordSA. Accessed in March 2023.
- [18] M. Ueda, S. Anzai and T. Kubo, Progressive crushing of a unidirectional CFRP plate with V-shaped trigger, *Advanced Composite Materials*, **24**, 2015, pp. 85-95.
- [19] VUMAT for Fabric Reinforced Composites (Abaqus Technical Document). Dassault Systèmes 2008.
- [20] A. Turon, C. Davila, P. Camanho and J. Costa, An engineering solution for mesh size effects in the simulation of delamination using Cohesive Zone Models. *Engineering Fracture Mechanics*, **74**, 2007, pp. 1665-1682.
- [21] P. P. Camanho, C. G. Davila, M. F. De Moura, Numerical simulation of mixed-mode progressive delamination in composite materials. *Journal of Composite Materials*, **37**, 2003, pp. 1415-1438.
- [22] C. McGregor, R. Vaziri, X. Xiao, Finite element modelling of the progressive crushing of braided composite tubes under axial impact, *International Journal of Impact Engineering*, **37**, 2010, pp. 662-672.
- [23] Q. Liu Q, J. Fu, Y. Ma, Y. Zhang and Q. Li, Crushing responses and energy absorption behaviors of multi-cell CFRP tubes, *Thin-Walled Structures*, **155**, 2020, p. 106930.